JCB Article

Regulation of Notch signaling by *Drosophila* heparan sulfate 3-*O* sulfotransferase

Keisuke Kamimura,[1,2] John M. Rhodes,[3] Ryu Ueda,[4] Melissa McNeely,[5] Deepak Shukla,[5] Koji Kimata,[2] Patricia G. Spear,[5] Nicholas W. Shworak,[3] and Hiroshi Nakato[1]

[1]Department of Genetics, Cell Biology, and Development, University of Minnesota, Minneapolis, MN 55455
[2]Institute for Molecular Science of Medicine, Aichi Medical University, Nagakute, Aichi 480-1195, Japan
[3]Section of Cardiology and Angiogenesis Research Center, Department of Medicine, Dartmouth Medical School, Dartmouth Hitchcock Medical Center, Lebanon, NH 03756
[4]Invertebrate Genetics Laboratory, Genetic Strain Research Center, National Institute of Genetics, Mishima, Shizuoka 411-8540, Japan
[5]Department of Microbiology-Immunology, Feinberg School of Medicine, Northwestern University, Chicago, IL 60611

Heparan sulfate (HS) regulates the activity of various ligands and is involved in molecular recognition events on the cell surface and in the extracellular matrix. Specific binding of HS to different ligand proteins depends on the sulfation pattern of HS. For example, the interaction between antithrombin and a particular 3-*O* sulfated HS motif is thought to modulate blood coagulation. However, a recent study of mice defective for this modification suggested that 3-*O* sulfation plays other biological roles. Here, we show that *Drosophila melanogaster HS 3-O sulfotransferase-b* (*Hs3st-B*), which catalyzes HS 3-*O* sulfation, is a novel component of the Notch pathway. Reduction of *Hs3st-B* function by transgenic RNA interference compromised Notch signaling, producing neurogenic phenotypes. We also show that levels of Notch protein on the cell surface were markedly decreased by loss of *Hs3st-B*. These findings suggest that *Hs3st-B* is involved in Notch signaling by affecting stability or intracellular trafficking of Notch protein.

Introduction

Heparan sulfate proteoglycans (HSPGs), abundant components of the cell surface and the extracellular matrix, are critically involved in a variety of biological phenomena, including cell adhesion, proliferation, and differentiation. The diverse functions of HSPGs are thought to be mediated by highly specific interactions between various binding proteins and distinct sequence motifs of the heparan sulfate (HS) chains. Such specific structures are predominantly determined by the regulated positioning of *N*-, 2-, 6-, and 3-*O* sulfate groups along the HS chains (for review see Esko and Selleck, 2002). For example, FGF-2 requires both *N*- and 2-*O* sulfate groups for binding to HS. The 6-*O* sulfate group is not essential for binding to FGF, but is critical for activation of the FGF receptor (for review see Nakato and Kimata, 2002). In contrast, binding of platelet-derived growth factor, hepatocyte growth factor, lipoprotein lipase, and herpes simplex virus (HSV) glycoprotein C to HS are all dependent on 6-*O* sulfation (for review see Lindahl et al., 1998). Thus, the biological functions of HSPGs are controlled by biosynthetic events that define the fine structures of HS.

The first and still the most notable example showing the importance of sequence-specific sulfation in HS–protein interactions comes from analyses of 3-*O* sulfated HS. The 3-*O* sulfate group is the rarest component in HS, and 3-*O* sulfation occurs late in the HS biosynthesis pathway (for review

The online version of this article includes supplemental material.

Address correspondence to Hiroshi Nakato, Dept. of Genetics, Cell Biology, and Development, University of Minnesota, 6-160 Jackson Hall, 321 Church St. SE, Minneapolis, MN 55455. Tel.: (612) 625-1727. Fax: (612) 626-5652. email: nakat003@umn.edu

D. Shukla's present address is Dept. of Ophthalmology and Visual Sciences, University of Illinois at Chicago, Chicago, IL 60612.

Key words: 3-*O* sulfation; heparan sulfate proteoglycan; Notch signaling; transgenic RNAi; *Drosophila*

Abbreviations used in this paper: ACV, anterior cross vein; A/P, anterior–posterior; AT, antithrombin; BDGP, Berkeley *Drosophila* Genome Project; ct, *cut*; *Dl*, *Delta*; *dpp*, *decapentaplegic*; *dx*, *deltex*; D/V, dorsal–ventral; *E(spl)C*, *Enhancer of split Complex*; gD, glycoprotein D; HS, heparan sulfate; HS3ST, HS 3-*O* sulfotransferase; HSPG, HS proteoglycan; HSV, herpes simplex virus; IR, inverted repeat; *kuz*, *kuzbanian*; *N*, *Notch*; N^{ECD}, extracellular domain of N protein; *neur*, *neuralized*; N^{ICD}, intracellular domain of N protein; RNAi, RNA interference; *sca*, *scabrous*; *Ser*, *Serrate*; SMC, sensory organ mother cell; ST, sulfotransferase; *Su(H)*, *Suppressor of Hairless*; UAS, upstream activating sequence; *vg*, *vestigial*; *wg*, *wingless*.

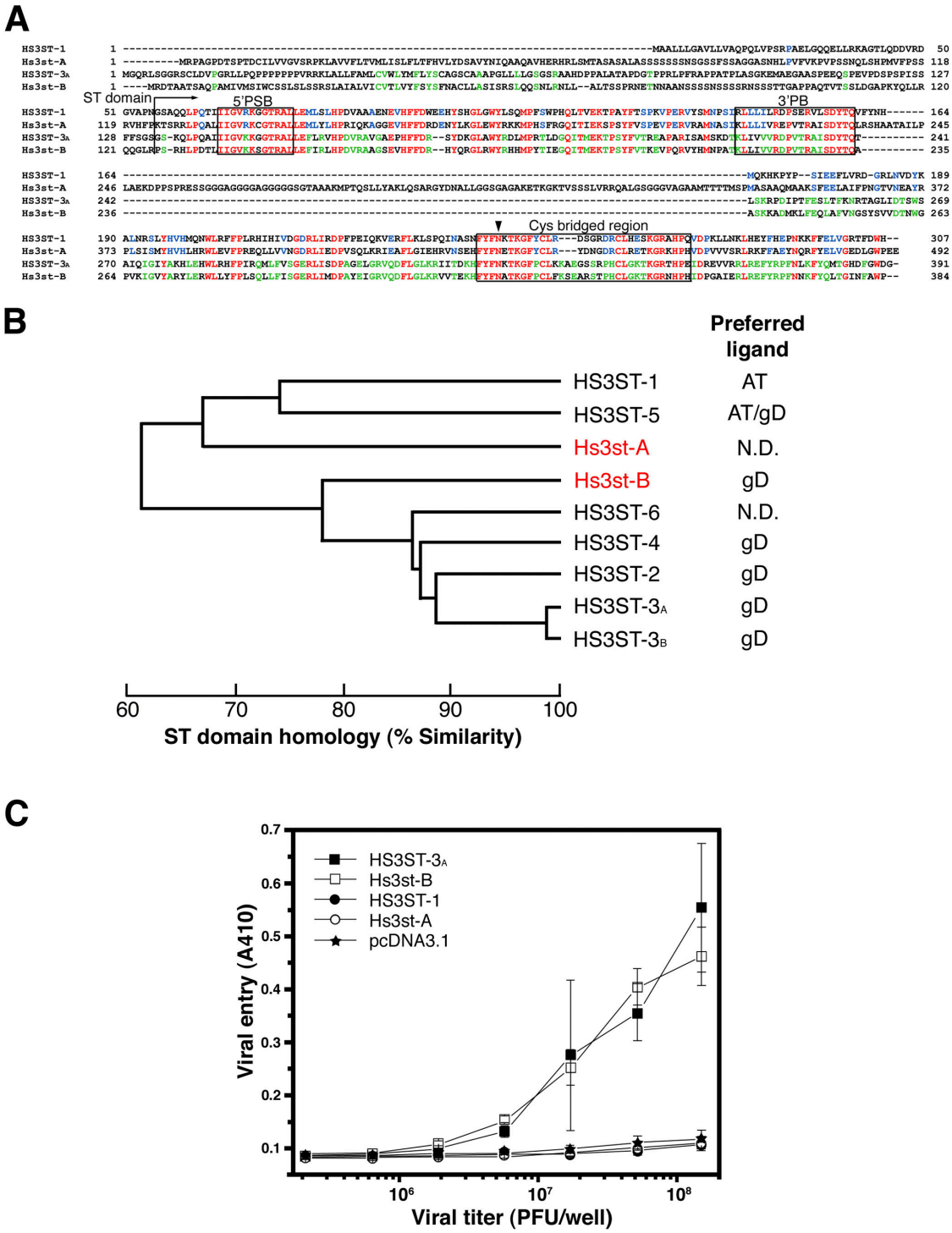

Figure 1. **Structures and enzymatic activities of *Drosophila* Hs3sts.** (A) Comparison of the amino acid sequences of human and *Drosophila* HS3STs. The program "Clustal W" was used to align amino acid sequences of human HS3STs and *Drosophila* Hs3sts. Consensus residues among four HS3STs are colored red. Identical residues between HS3ST-1 and Hs3st-A and between $HS3ST\text{-}3_A$ and Hs3st-B are marked in blue and green, respectively. The arrowhead indicates the potential *N*-glycosylation signal conserved in all HS3STs. (B) A dendrogram comparing sulfotransferase (ST) domains from all human and *Drosophila* isoforms. The dendrogram was generated by calculating the average similarity of amino acid sequences of the ST domain as determined by the University of Wisconsin Genetics Computer Group program "Distances" (Shworak et al., 1999). The preferred ligands of HS treated with HS3ST-1 (Shworak et al., 1997), $HS3ST\text{-}3_A$ (Shukla et al., 1999), $HS3ST\text{-}3_B$ (Shukla et al., 1999), HS3ST-2, HS3ST-4 (unpublished data), and HS3ST-5 (Xia et al., 2002; HajMohammadi et al., 2003) are shown. *Drosophila* Hs3sts are colored red. The HS3ST multigene family is comprised of two structurally distinct groups. The following information for amino acid sequences of human HS3STs was used: GenBank/EMBL/DDBJ accession no. AF019386 (HS3ST-1), AF105374 (HS3ST-2), AF105376 ($HS3ST\text{-}3_A$), AF105377 ($HS3ST\text{-}3_B$), AF105378 (HS3ST-4), AF50392 (HS3ST-5), and the unpublished sequence for HS3ST-6 (unpublished data). (C) Enzymatic sequence specificity of Hs3st-B. Generation of functional HS^{gD+} was assessed by transfecting CHO cells with the indicated plasmids. Transfectants were exposed to various concentrations of HSV-1(KOS)tk12 (Warner et al., 1998), which expresses

see Rosenberg et al., 1997). In humans, there are at least seven HS 3-*O* sulfotransferases (HS3STs) that produce at least two distinct forms of 3-*O* sulfated HS (Shworak et al., 1997, 1999; Shukla et al., 1999; Xia et al., 2002). One form of 3-*O* sulfated HS plays a critical role in the blood coagulation cascade. HS3ST-1 generates HS^{AT+}: HS with a specific 3-*O* sulfated motif that binds to antithrombin (AT). In therapeutic heparin administration, this interaction leads to inactivation of thrombin, resulting in inhibition of blood coagulation (Rosenberg et al., 1997; Shworak et al., 1997). However, a recent report showed that *Hs3st1*$^{-/-}$ knockout mice do not exhibit an obvious procoagulant phenotype even though HS^{AT+} levels in these mice are largely reduced (HajMohammadi et al., 2003). Instead, these mice showed postnatal lethality and intrauterine growth retardation, implying other physiological roles for 3-*O* sulfation. A different form of 3-*O* sulfated HS is involved in the entry of HSV-1 into host cells and the fusion of infected cells. HS3ST-3 isoforms generate HS^{gD+}: HS with a different 3-*O* sulfated sequence that mediates the cellular entry of HSV-1. HS^{gD+} on the surface of animal cells interacts with a viral coat protein, glycoprotein D (gD), to promote fusion of the HSV-1 envelope with the cell membrane of host cells (Shukla et al., 1999). Multinucleated giant cells (polykaryocytes), resulting from virus-induced cell fusion, are a hallmark of HSV-1 infection. It has also been demonstrated that CHO cells expressing HS3ST-3 fuse with CHO cells that express viral glycoproteins gB, gD, gH, and gL, suggesting that 3-*O* sulfated HS has a crucial role both in the entry and spreading of HSV-1 (Tiwari et al., 2004). However, an endogenous ligand for this HS sequence is not known. Thus, although sequence-specific 3-*O* sulfation clearly has key roles in defining interactions between HS and specific binding proteins, its in vivo relevance is poorly understood. Interestingly, sequences homologous to mammalian *HS3ST* genes are found in the genome of *Drosophila melanogaster* and *Caenorhabditis elegans* despite the very dissimilar blood coagulation systems that occur in lower animals. The existence of *HS3ST* homologues in these organisms suggests that 3-*O* sulfation has a role in evolutionarily conserved processes, such as the developmental pathways mediated by secreted factors or integral membrane proteins.

One of the central and widely deployed developmental pathways in the animal kingdom is Notch (N) signaling (for reviews see Panin and Irvine, 1998; Artavanis-Tsakonas et al., 1999; Mumm and Kopan, 2000; Baron et al., 2002). In *Drosophila*, the core components of this pathway are the receptor N, and the ligands Delta (Dl) and Serrate (Ser). Upon binding the ligands, N undergoes Presenilin-dependent processing, which results in the release of the intracellular domain of N (N^{ICD}) from the membrane. Subsequently, this domain translocates to the nucleus where it forms a complex with Suppressor of Hairless (Su(H)) and Mastermind to activate the expression of target genes such as *Enhancer of split Complex* (*E(spl)C*). During maturation of N protein, this molecule undergoes extensive modulation mediated by various molecules such as a glycosyltransferase, Fringe; extracellular modulator, Scabrous (Sca); and metalloproteinase, Kuzbanian (Kuz). Furthermore, proper transport to the cell surface as well as internalization of N protein are required for the normal activity of this molecule. Multiple genes are known to affect N signaling through roles in membrane trafficking. These include Shibire (dynamin), Ca-P60A (Ca^{2+} ATPase), heatshock cognate 70, Warthog (rab6), Numb, and *N*-ethylmaleimide–sensitive fusion protein (for review see Baron et al., 2002).

To examine the in vivo importance of a specific sulfation of HS for the interaction with binding proteins, we studied the function of 3-*O* sulfated HS during *Drosophila* development. We isolated cDNA clones for two *Drosophila Hs3sts* (*Hs3st-A* and *-B*), and characterized their structures, expression, and functions. Transfectional analyses showed that Hs3st-B, like HS3ST-3 isoforms, mediated cellular entry of HSV-1 that is triggered by HS^{gD+}. We found that reduction of *Hs3st-B* function using the transgenic RNA interference (RNAi) technique caused neurogenic phenotypes that are characteristic of N signaling mutants. *Hs3st-B* genetically interacts with various N signaling components and regulates expression of *N* target genes. In addition, levels of N protein were markedly decreased by reduction of *Hs3st-B*. These findings show that Hs3st-B is a novel regulator of the N signaling pathway and controls pattern formation. We also observed that the *Hs3st-B* RNAi affects the number and size of endosomal/lysosomal compartments, suggesting the role of 3-*O* sulfated HS in intracellular trafficking of N protein.

Results

Primary structures and enzymatic activities of *Drosophila* Hs3sts

Blast homology searches of the *Drosophila* genome identified two genes (CG33147 and CG7890) closely related to mammalian HS3STs, which we named *Drosophila Hs3st-A* and *-B* (Shworak et al., 1997, 1999). To analyze the structures of these molecules, we obtained an *Hs3st-A* cDNA clone (GH20068) from the Berkeley *Drosophila* Genome Project (BDGP) and an *Hs3st-B* cDNA clone by screening a *Drosophila* embryonic cDNA library using an *Hs3st-B* genomic DNA fragment as a probe (Brown and Kafatos, 1988). The deduced amino acid sequences of the *Hs3sts* encoded type-II integral membrane proteins, which is typical of Golgi enzymes (unpublished data). The Hs3sts also showed characteristic motifs conserved among all mammalian HS3STs, including binding sites for 3′-phosphoadenosine 5′-phosphosulfate, cysteine-bridged regions, and *N*-glycosylation sites (Fig. 1 A; Shworak et al., 1999).

Most importantly, mammalian HS3STs share a highly conserved COOH-terminal region known as the sulfo-

β-galactosidase from an insert in the viral genome. β-Galactosidase activity, a measure of viral entry, was quantified at 6 h after the addition of virus. Representative values from a single transfection show the amount of reaction product detected spectrophotometrically (A_{410}) as the mean ± SD from three wells per virus dose (PFU, plaque forming units). Comparable results were obtained in three independent transfection experiments. 5′PSB, 5′-phosphosulfate binding site; 3′PB, 3′-phosphate binding site; N.D., not determined.

transferase (ST) domain (Shworak et al., 1997, 1999). Homology comparison of the ST domains of human and *Drosophila* HS3STs indicated two major groups of enzymes with a single *Drosophila* isoform parsing into each group (Fig. 1 B). Hs3st-A was most similar to HS3ST-1 and -5, which both generate HS^{AT+} (Fig. 1 B; Shworak et al., 1997; Xia et al., 2002). Conversely, Hs3st-B was related to the remaining enzymes, many of which are known to preferentially generate HS^{gD+} (Fig. 1 B; Shukla et al., 1999; unpublished data). Substrate specificity of the HS3STs is determined by the structure of the ST domain (Yabe et al., 2001); thus, the homology analysis predicts that Hs3st-A and Hs3st-B might produce different 3-*O* sulfated HS structures for distinct binding proteins. However, structural similarities do not completely predict enzymatic specificities, as HS3ST-5 can also produce HS^{gD+} and HS3ST-3_A can make low levels of HS^{AT+} (Yabe et al., 2001; Xia et al., 2002). Consequently, we analyzed enzymatic specificities of Hs3sts.

We subcloned *Drosophila* and representative mammalian HS3ST cDNAs into the pcDNA3.1 expression vector and determined the enzymatic ability to create functional HS^{gD+} by an in vivo assay in which the sequence specific activity of HS3ST-3 isoforms generates HS^{gD+} and renders CHO cells susceptible to infection by HSV-1 (Shukla et al., 1999). Thus, CHO cells were transfected with HS3ST expression constructs, and then exposed to a recombinant form of HSV-1, and virus entry was monitored (Fig. 1 C). Negligible viral entry was detected in cells expressing Hs3st-A, the empty vector control, or HS3ST-1, which does not produce HS^{gD+} (Shukla et al., 1999). In contrast, expression of Hs3st-B conveyed cellular susceptibility to HSV-1 entry, as did the HS3ST-3_A–positive control. Moreover, coexpression of HSV-1 gD with Hs3st-B reduced cellular susceptibility (unpublished data) through the ability of cellular gD to interfere with viral entry via HS^{gD+} (Shukla et al., 1999). Together, these results demonstrate that Hs3st-B, like HS3ST-3_A, preferentially generates HS^{gD+}. Thus, the two *Drosophila* HS3ST enzymes exhibit distinct yet phylogenetically conserved sequence specificities.

mRNA expression of *Hs3sts*

To determine the temporal and spatial expression pattern of the *Hs3st* mRNAs, we performed RT-PCR and in situ RNA hybridization. RT-PCR revealed that *Hs3st-A* mRNA is expressed at low levels in all stages examined (Fig. 2 A). Its transcription levels were especially low in larval and pupal stages. In contrast, *Hs3st-B* mRNA is abundantly expressed throughout development (Fig. 2 A). We next examined the spatial distribution of *Hs3st-B* in embryos and larval imaginal tissues by in situ hybridization (Fig. 2 B). In these tissues, *Hs3st-B* was widely but not evenly expressed. *Hs3st-B* expression was particularly enriched in the salivary glands in embryos, the morphogenetic furrow of eye discs, and the brain lobes of the larval CNS. In the wing disc, *Hs3st-B* mRNA was detected at high levels in the wing pouch region (Fig. 2 C). We failed to detect any signals from *Hs3st-A* mRNA (unpublished data), probably due to the low level of expression.

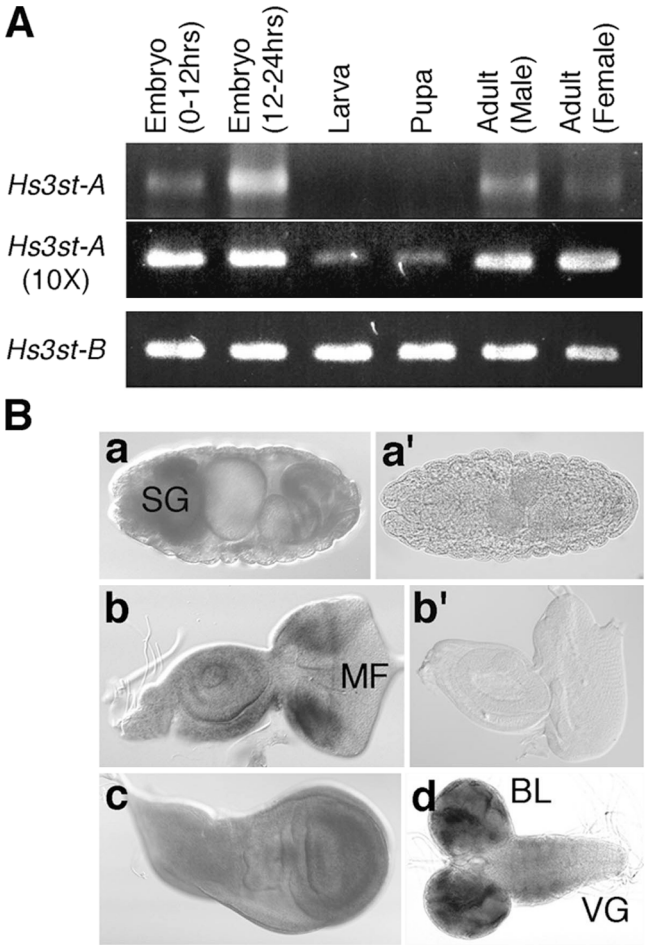

Figure 2. **mRNA expression of *Hs3st-A* and *-B*.** (A) Temporal expression pattern of *Hs3st* mRNAs. Total RNA samples were prepared from the indicated developmental stages, and expression of *Hs3st-A* and *Hs3st-B* was examined by RT-PCR. For *Hs3st-A*, we also performed RT-PCR using a 10-fold higher concentration of cDNA template to detect low levels of expression at larval and pupal stages (10×). (B) In situ RNA hybridization of *Hs3st-B* mRNA in the embryo (stage 16, a), eye disc (b), wing disc (c), and larval CNS (d). Embryo (stage 16, a′) and eye disc (b′) stained with a sense strand probe are shown. In these figures, anterior is left (a, a′, b, b′, and d) or up (c). In the embryo, enriched expression was detected in the salivary gland. In third instar larvae, high levels of expression were detected in the brain lobe and the morphogenetic furrow of the eye disc. SG, salivary gland; MF, morphogenetic furrow; BL, brain lobe; VG, ventral ganglion.

Hs3st-B transgenic RNAi flies show neurogenic phenotypes

To elucidate the function of the *Hs3st* genes, it is critical to know the loss-of-function phenotypes of animals in which the activities of Hs3sts are compromised. However, there are no mutations identified in these loci. Therefore, we used the transgenic RNAi technique to analyze the in vivo function of *Hs3st-A* and *-B* (Kennerdell and Carthew, 2000). In this method, a hairpin RNA is expressed from a transgene exhibiting dyad symmetry under the control of GAL4 drivers. Expressed RNAs are double stranded and selectively interfere with expression of the specific target genes. This method has been successfully applied for functional analyses of nu-

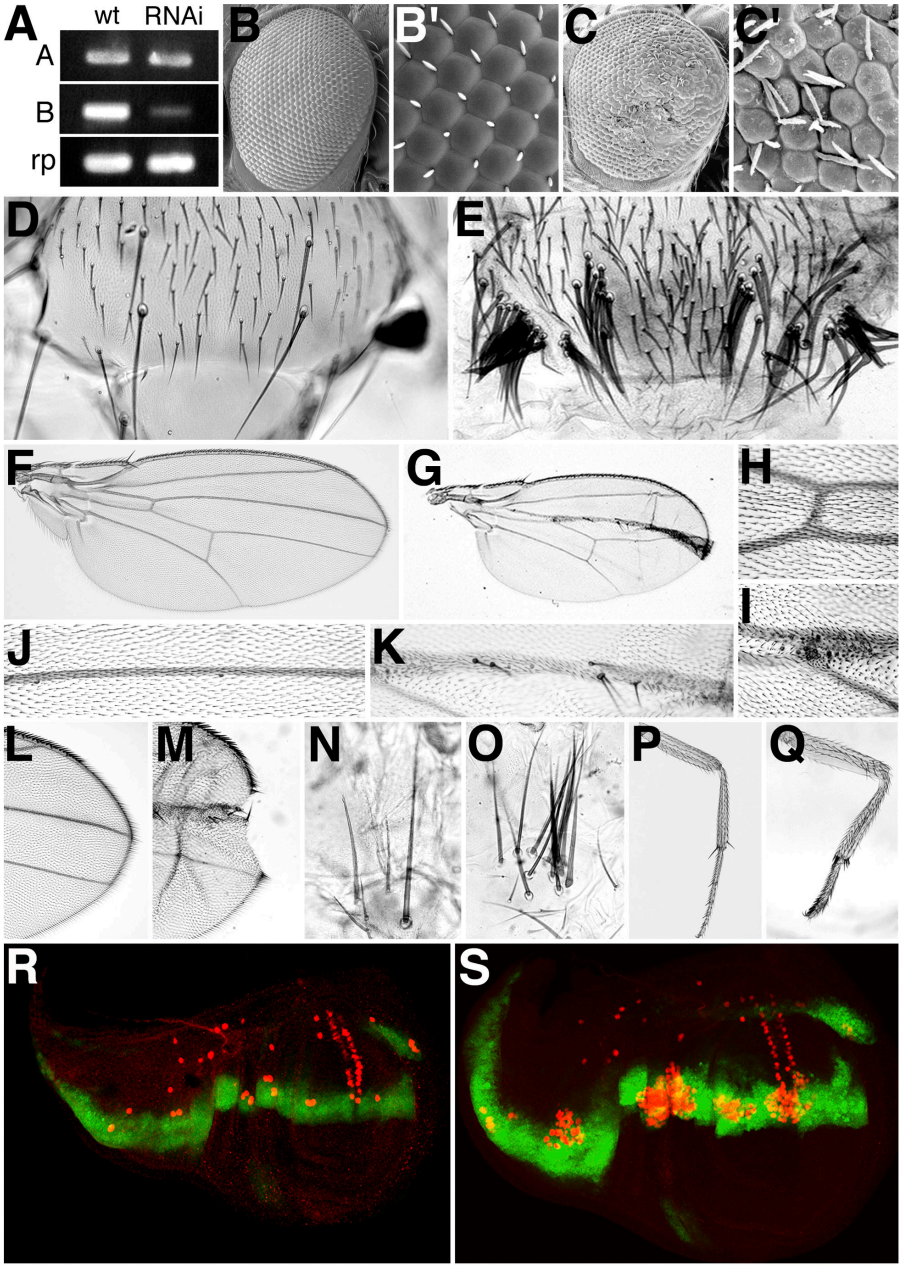

Figure 3. ***Hs3st-B* transgenic RNAi produced neurogenic phenotypes.** (A) RT-PCR analyses showing expression of *Hs3st-A* (A), *Hs3st-B* (B), and *ribosomal protein 49* (rp) mRNAs in third instar larvae from wild-type (wt) and *Hs3st-B* transgenic RNAi (RNAi) animals. Expression of *IR-Hs3st-B* using *actin-GAL4* specifically reduced *Hs3st-B* mRNA level. (B–S) Phenotypes of control animals (*GMR-GAL4/+*, B and B′; *dpp-GAL4/+*, D, F, H, J, L, N, P, and R) and *Hs3st-B* transgenic RNAi (*GMR-GAL4/UAS-IR-Hs3st-B*, C and C′; *UAS-IR-Hs3st-B/+*; *dpp-GAL4/+*, E, G, I, K, M, O, Q, and S) animals. (B, B′, C, and C′) Scanning EM of adult eyes. B′ and C′ show a high magnification view of adult eye for B and C, respectively. *Hs3st-B* transgenic RNAi caused necrotic death or fusion of ommatidia and duplication or loss of interommatidial bristles (C and C′). (D and E) Adult nota. (F–M) Adult wings. H and I show a high magnification view of the ACV for F and G, respectively. J and K show a high magnification view of wing vein L3 for F and G, respectively. L and M show the distal region of the wing. (N–Q) Bristles on the sternopleura, a part of the lateral thorax (N and O) and on the leg (P and Q). In the wing, *Hs3st-B* transgenic RNAi caused reduction of wing size (G), loss of the ACV (I), thickening of wing vein L3 (K), extra or ectopic sensory organs on ACV (I) and L3 vein (K), and notching at the wing margin (M). Extra sensory bristles were also observed on the notum (E), sternopleura (O), and leg (Q). Expression of *IR-Hs3st-B* also disrupts the joints between tarsal segments, leading to shortened legs (Q). (R and S) SMCs were labeled by expression of *neur-lacZ* (red) in *dpp-GAL4, UAS-GFP/neur-lacZ* (R) and *UAS-IR-Hs3st-B/+*; *dpp-GAL4, UAS-GFP/neur-lacZ* wing discs (S). In these figures, anterior of wing disc is up and dorsal is left. The number of SMCs for chemosensory bristles in the A/P boundary marked by GFP were dramatically increased in *IR-Hs3st-B* animals. We did not observe these defects in any control animals (*UAS-IR-Hs3st-B/+*, *GMR-GAL4/+*, or *dpp-GAL4/+*).

merous genes (Ueda, 2001). We established transgenic fly strains bearing inverted repeats (IRs) of 500 bp DNA sequences corresponding to the NH_2 terminus of *Hs3st* coding regions under the control of upstream activating sequences (UAS) for the GAL4 transcription factor (*UAS-IR-Hs3st-A* and *-B*; Brand and Perrimon, 1993). Expression of either *IR-Hs3st-A* or *-B* using ubiquitous drivers such as *actin-GAL4* caused strong lethality during embryonic and larval stages, showing that *Hs3st-A* and *-B* are critically required for viability (unpublished data).

In this work, we focused our analysis on the function of *Hs3st-B*. To test the effectiveness of *Hs3st-B* transgenic RNAi, we examined the ability of *IR-Hs3st-B* to reduce endogenous *Hs3st-B* mRNA expression. To prepare RNA from *actin-GAL4/UAS-IR-Hs3st-B* animals, larval stages were reared at 18°C, and then shifted to 25°C for 24 h before RNA preparation. RT-PCR analysis showed that expression of *UAS-IR-Hs3st-B* dramatically reduced the *Hs3st-B* mRNA level, whereas it had no effect on mRNA levels of *Hs3st-A* and *ribosomal protein 49* (Fig. 3 A), confirming the target specificity of the transgenic RNAi technique.

We found that tissue-specific expression of *UAS-IR-Hs3st-B* using several GAL4 drivers caused a variety of morphological defects. For example, expression of *UAS-IR-Hs3st-B* under the control of *GMR-GAL4*, an eye-specific driver, caused a severe rough eye phenotype, including an irregular array or fusion of ommatidia and duplication or loss of interommatidial bristles (Fig. 3, C and C′). Expres-

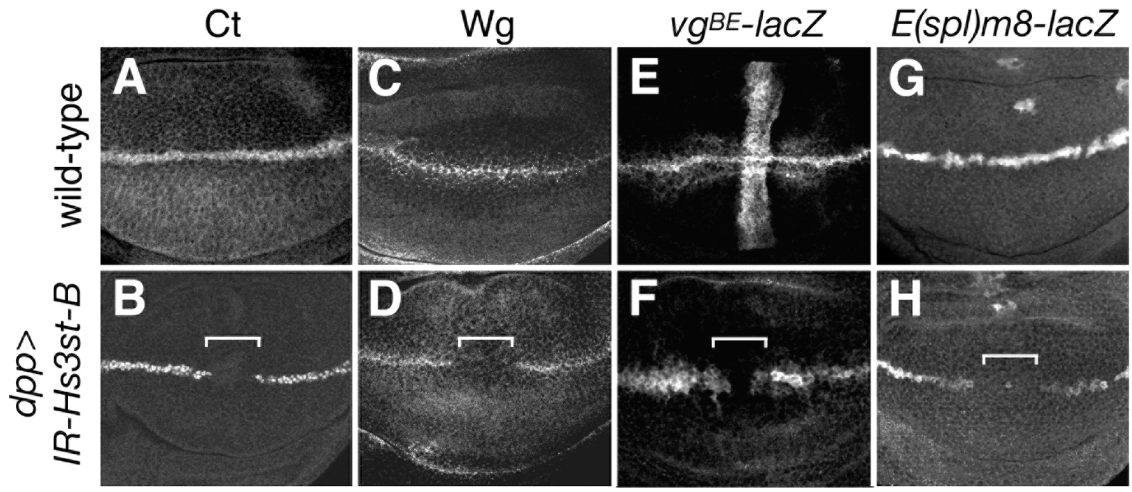

Figure 4. **Expression of *N* target genes was eliminated by reduction of *Hs3st-B* function.** Antibody staining of wing discs from control (A, C, E, and G) and the *Hs3st-B* RNAi (B, D, F, and H) animals. Wing discs for wild-type (A and C) and *UAS-IR-Hs3st-B/+*; *dpp-GAL4/+* (B and D) were stained for Ct (A and B) and Wg (C and D), respectively. Enhancer activity for *vg* (E and F) and *E(spl)m8* gene (G and H) were examined in vg^{BE}*-lacZ/+* (E), vg^{BE}*-lacZ/UAS-IR-Hs3st-B*; *dpp-GAL4/+* (F), *E(spl)m8-lacZ/+* (G), and *E(spl)m8-lacZ/UAS-IR-Hs3st-B*; *dpp-GAL4/+* (H) wing discs. Expression of *IR-Hs3st-B* under the control of *dpp-GAL4* abolished expression of these *N* target genes along the A/P boundary (B, D, F, and H, bracket). In this and subsequent figures, anterior of the wing disc is left and dorsal is up.

sion of *UAS-IR-Hs3st-B* driven by *decapentaplegic* (*dpp*)*-GAL4* produced several characteristic phenotypes in adult tissues, including numerous ectopic sensory bristles (macrochaetae) on the mesothoratic notum (Fig. 3 E). The *Hs3st-B* RNAi also caused reduction of wing size (Fig. 3 G), loss of the anterior cross vein (ACV; Fig. 3 I), thickening of wing vein L3 (Fig. 3 K), extra or ectopic sensory organs on the ACV and vein L3 (Fig. 3, I and K), and notching at the wing margin (Fig. 3 M). Extra sensory bristles were also observed on sternopleura (Fig. 3 O) and legs (Fig. 3 Q). Expression of *IR-Hs3st-B* at the anterior–posterior (A/P) boundary using *patched-GAL4* produced similar morphological defects, indicating that these phenotypes are not dependent on a specific GAL4 driver. The observed phenotypes are characteristic of a reduced activity of neurogenic genes such as components of the N signaling pathway (Lehmann et al., 1981, 1983). During the formation of sensory organ bristles, an N-mediated process called "lateral inhibition" singles out a sensory organ mother cell (SMC) from the proneural cluster (Simpson, 1990). Anti–β-galactosidase antibody staining for the SMC-specific marker *neuralized* (*neur*)*-lacZ* in the *Hs3st-B* transgenic RNAi wing discs revealed numerous SMCs from each proneural cluster (Fig. 3 S), suggesting that N-mediated lateral inhibition is disturbed in these animals. Some of the phenotypes that *Hs3st-B* transgenic RNAi produced are common to those resulting from defective growth factor signaling systems, including Hedgehog, Dpp, and Wingless (Wg). However, several features suggest that *Hs3st-B* specifically affects N signaling. For example, *Hs3st-B* transgenic RNAi produces segmental fusions of the leg that are similar to *N* mutant phenotypes but different from those caused by *hedgehog*, *dpp*, and *wg* mutations (Fig. 3 Q; Goto et al., 2001). In addition, expression of *IR-Hs3st-B* in the wing discs does not affect expression of Hedgehog target genes, such as *patched* and *dpp* (unpublished data). Together, these results raise the possibility that *Hs3st-B* is involved in N signaling. This finding was further confirmed by analysis of the genetic interactions between *Hs3st-B* and N signaling components. *Hs3st-B* showed strong genetic interactions with various N pathway genes such as *N*, *Dl*, *sca*, *kuz*, and *deltex* (*dx*), suggesting that *Hs3st-B* participates in the N pathway (see supplemental data, available at http://www.jcb.org/cgi/content/jcb.200403077/DC1).

Hs3st-B regulates N target genes during wing margin formation

During wing development, the N pathway activates a set of genes controlling wing margin formation, such as *cut* (*ct*), *wg*, and *vestigial* (*vg*), in a stripe of cells along the dorsal–ventral (D/V) boundary (Fig. 4, A, C, and E; Couso et al., 1995; Kim et al., 1995; Rulifson and Blair, 1995; Micchelli et al., 1997). To ask if *Hs3st-B* regulates N signaling, we examined expression of Ct, Wg, and the *vg* boundary enhancer, vg^{BE}*-lacZ,* in the *Hs3st-B* transgenic RNAi animals. Expression of *IR-Hs3st-B* under the control of *dpp-GAL4* completely eliminated expression of these genes in the central region of the disc (Fig. 4, B, D, and F). We also examined expression of *E(spl)m8,* the *m8* gene from *E(spl)C,* which is induced along the D/V boundary by N signaling, although *E(spl)m8* is not required for wing margin formation (Fig. 4 G; de Celis et al., 1996). We found that the *Hs3st-B* transgenic RNAi also abolished *E(spl)m8-lacZ* expression (Fig. 4 H). Because transcription of *vg* and *E(spl)m8* along the D/V boundary is induced by direct interaction between their regulatory sequences and Su(H) DNA binding protein (Lecourtois and Schweisguth, 1995; Kim et al., 1996), our results suggest that *Hs3st-B* is required for the Su(H)-mediated N pathway. Thus, *Hs3st-B* regulates N signaling during wing margin formation, which is consistent with its phenotypic effects and genetic interactions.

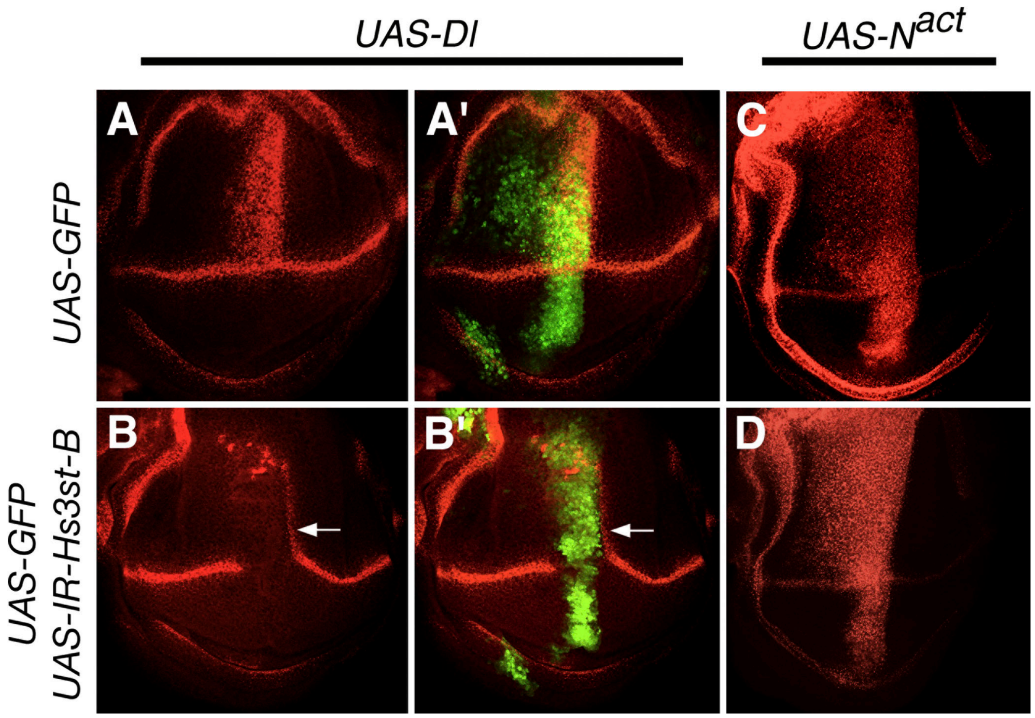

Figure 5. ***Hs3st-B* acts downstream of Dl and upstream of N.** (A and A′) Wing disc from a *dpp-GAL4 UAS-GFP/UAS-Dl* larva stained with anti-Wg antibody (red). Ectopic Dl expression using *dpp-GAL4* (marked by GFP; A′, green) induces Wg expression along the A/P boundary in the dorsal compartment. (B and B′) Expression of Wg protein (red) and GFP (B′, green) is shown for *UAS-IR-Hs3st-B/+; dpp-GAL4 UAS-GFP/UAS-Dl*. Coexpression of *IR-Hs3st-B* with *Dl* completely suppressed *Dl*-dependent ectopic expression of Wg in *IR-Hs3st-B*–expressing cells but not in the adjacent cells (arrows, compare with A′). (C) A *dpp-GAL4/UAS-N^{act}* wing disc stained for Wg protein (red). Expression of the activated form of N (N^{act}) using the same GAL4 driver causes ectopic expression of Wg at the A/P border in both the dorsal and ventral compartment. (D) A *UAS-IR-Hs3st-B/+; dpp-GAL4/UAS-N^{act}* disc stained for Wg protein (red). Ectopic activation of Wg induced by N^{act} expression was not affected by the *Hs3st-B* transgenic RNAi (compare with C).

Hs3st-B acts downstream of *Dl* expression and upstream of N activation

To determine the specific step of N signaling that requires 3-*O* sulfated HS, we analyzed the genetic epistasis of *Hs3st-B* in the signaling. As mentioned in the previous paragraph, N signaling induces target genes such as *wg* along the D/V boundary during wing margin formation (Fig. 4 C). Ectopic activation of N results in misexpression of these target genes. For example, when the N ligand Dl is ectopically expressed using *UAS-Dl (30B)* under the control of *dpp-GAL4*, expression of Wg protein is induced along the A/P boundary in the dorsal compartment (Fig. 5, A and A′; Kim et al., 1995; Doherty et al., 1996). We found that this *Dl*-dependent Wg expression was repressed by the *Hs3st-B* transgenic RNAi (Fig. 5, B and B′). In contrast, expression of an activated form of the receptor N (N^{act}; lacking extracellular domain of N [N^{ECD}]) by *dpp-GAL4* results in ectopic activation of Wg at the A/P border in both dorsal and ventral compartments (Fig. 5 C; Doherty et al., 1996). This ectopic Wg induced by N^{act} was not affected by coexpression of *IR-Hs3st-B* (Fig. 5 D). These results indicate that *Hs3st-B* functions downstream of *Dl* transcription but upstream of N activation.

These experiments also provided information on the cell autonomy of *Hs3st-B* function. Because activation of N signaling by Dl occurs nonautonomously, ectopic expression of Wg is induced outside *Dl*-expressing cells (Fig. 5, A and A′; Doherty et al., 1996). As depicted in Fig. 5 (B and B′), expression of *IR-Hs3st-B* abolished Wg expression only in a cell autonomous fashion and did not affect Wg expression in the neighboring cells (Fig. 5, arrows). This observation shows that (a) *Hs3st-B* activity is autonomously required only in the signal receiving cells but not in the signal sending cells, and (b) *Hs3st-B* RNAi does not affect the activity of Dl itself expressed by *UAS-Dl* transgene.

Hs3st-B transgenic RNAi affects N protein levels

The activity of N protein is regulated at multiple steps including proteolytic processing, glycosylation, intracellular transport to the cell surface, and degradation (for review see Baron et al., 2002). To gain insight into the mechanism for control of N function by *Hs3st-B*, we examined N protein distribution in wing discs from *Hs3st-B* transgenic RNAi animals using antibodies against the N^{ECD} or N^{ICD}. In the third instar larva of wild type, N is evenly expressed throughout the wing disc with the highest protein levels on the apical surface (Fig. 6, A and C; Fehon et al., 1991). We found that expression of *IR-Hs3st-B* by *dpp-GAL4* significantly reduced signals for both N^{ECD} (Fig. 6, B and B′) and N^{ICD} (Fig. 6, D and D′) at the A/P boundary. The reduction of N protein levels was not caused by decreased expression of the *N* gene because *Hs3st-B* RNAi did not affect levels and patterns of *N-lacZ* expression in the wing disc (Fig. 6, F and F′; de Celis et al., 1997).

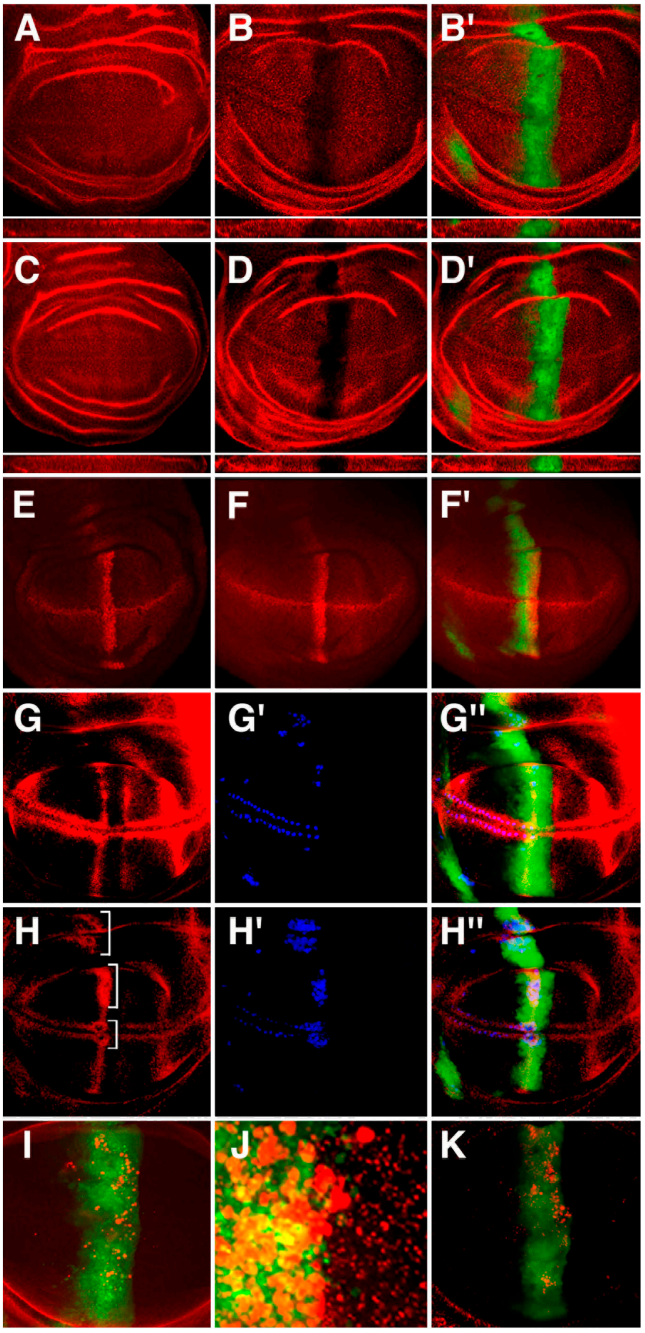

Figure 6. ***Hs3st-B* transgenic RNAi affects N protein levels.** Wing discs from wild-type (A and C) and *UAS-IR-Hs3st-B/+; dpp-GAL4 UAS-GFP/+* larvae (B, B′, D, and D′) stained with anti-N^{ECD} (A–B′, red) or anti-N^{ICD} (C–D′, red). Cross sections near the D/V boundary are shown at the bottom of each panel (apical side is up). *Hs3st-B* transgenic RNAi markedly reduced signals for epitopes in both N^{ECD} and N^{ICD}. (E–F′) Wing discs from N^{MLz}*-lacZ/+* (E) and N^{MLz}*-lacZ/+; UAS-IR-Hs3st-B/+; dpp-GAL4 UAS-GFP/+* (F and F′) larvae stained with anti–β-galactosidase antibody (red). Expression of N^{MLz}*-lacZ* was detected strongly at the A/P and D/V compartment boundary (E). This pattern was not affected by the *Hs3st-B* RNAi (F and F′). (G–H″) Wing discs from *dpp-GAL4 UAS-GFP/neur-lacZ* (G–G″) and *UAS-IR-Hs3st-B/+; dpp-GAL4 UAS-GFP/neur-lacZ* larvae (H–H″) stained with anti-Dl antibody (red). In wild-type background, Dl protein is detectable in prevein regions, stripes of cells flanking the D/V boundary, and around SMCs (G). *neur-lacZ* marks the location of SMCs (G′, blue). *Hs3st-B* RNAi did not affect gross patterns of Dl expression, but increased local levels of Dl protein around SMCs (H, brackets). Note that the number of SMCs is increased as shown in Fig. 3 S (H′, blue). (I and J) Wing discs from *UAS-IR-Hs3st-B/+; dpp-GAL4 UAS-GFP/+* larvae showing late endosomes visualized by Texas red dextran internalization (red). Expression of *IR-Hs3st-B* increased the number and size of late endosomes. J shows a high magnification view of a different wing disc with the same genotype as I. (K) Lysosomes are labeled in a *UAS-IR-Hs3st-B/+; dpp-GAL4 UAS-GFP/+* wing disc using LysoTracker (red). *Hs3st-B* RNAi causes increased and enlarged lysosomes. Expression patterns of *dpp-GAL4* are marked by GFP (B′, D′, F′, G″, H″, I, J, and K, green).

Previous papers have shown that high levels of N ligands Dl and Ser inhibit N signaling in a cell-autonomous fashion (Micchelli et al., 1997). To examine whether or not the reduction of N protein levels in *Hs3st-B* RNAi animals is caused by high levels of N ligands, we examined expression of Dl protein in these animals. In the wild-type wing discs at the late third instar, Dl is expressed in the prevein regions, stripes of cells flanking the D/V boundary, and around SMCs (Fig. 6, G–G″; Kooh et al., 1993). We found that *IR-Hs3st-B* expression did not affect the overall patterns of Dl expression, but did increase local levels of Dl protein around SMCs (Fig. 6, H–H″). This local up-regulation of Dl expression has been previously reported; in *N* mutant wing discs, high levels of Dl protein were observed at regions of proneural clusters (de Celis and Bray, 1997). This finding indicates that *Hs3st-B* RNAi directly decreases N protein levels and affects Dl expression locally as a secondary effect. Together, these findings suggest that *Hs3st-B* regulates the presentation of N on the cell surface or the stability of N protein.

Hs3st-B transgenic RNAi affects distribution and morphology of intracellular membrane compartments

Two lines of evidence prompted us to examine the effects of *Hs3st-B* RNAi on vesicle trafficking. First, several mutations in genes involved in intracellular trafficking or endocytosis compromise N signaling (for review see Baron et al., 2002). Second, a mammalian homologue of Hs3st-B, HS3ST-3, has a critical role in membrane fusion. 3-*O* sulfated HS generated by HS3ST-3 mediates fusion of the envelope of HSV-1 and the host cell membrane (Shukla et al., 1999). Furthermore, CHO cells expressing HS3ST-3 fuse with other CHO cells that express viral glycoproteins, resulting in the generation of polykaryocytes (Tiwari et al., 2004).

We studied the effects of *Hs3st-B* RNAi on the morphology of endosomal/lysosomal compartments. Wing discs from *Hs3st-B* RNAi animals (*UAS-IR-Hs3st-B/+; dpp-GAL4,UAS-GFP/+*) were cultured in medium containing an endocytosis marker (Texas red dextran) or a lysosomal marker (LysoTracker). We found that *IR-Hs3st-B* expression strikingly increased the number and size of both dextran and LysoTracker-uptaking vesicular puncta (Fig. 6, I–K). Such enlarged endosomal/lysosomal compartments may lead to a higher rate of protein degradation. We tested whether or not impairment of N signaling causes the same changes of the endosomal/lysosomal compartments and found that expression of either a dominant-negative form of *N* or an *N* transgenic RNAi construct driven by *dpp-GAL4* does not induce such phenomena (unpublished data). Thus, the changes in number and size of the endosomal/lysosomal compartments

seem to be directly induced by the *Hs3st-B* RNAi and not through a reduction of N signaling. In summary, these results suggested one possible mechanism in which reduction of N protein levels in *Hs3st-B* RNAi is caused by defects in trafficking to the cell surface and/or to the endosomal/lysosomal compartments.

Discussion

Function of 3-*O* sulfated HS in vivo

Several biochemical studies suggest that sulfation at specific positions of HS regulates intercellular signaling. However, the physiological significance of these sulfation events is still poorly understood. 3-*O* sulfation is one of the best studied examples showing the importance of specific fine structures in controlling the binding affinity of HS to selective ligands. 3-*O* sulfated HS produced by HS3ST-1 binds to AT (Shworak et al., 1997, 1999), and this interaction has been thought to be a key step in inhibiting blood coagulation. However, several lines of evidence suggest that 3-*O* sulfated HS also plays roles in evolutionarily fundamental systems such as developmental signaling. First, *Hs3st1*$^{-/-}$ mice showed postnatal lethality and intrauterine growth retardation without obvious effects on the blood coagulation (Haj-Mohammadi et al., 2003), suggesting that 3-*O* sulfated HS may serve other biological roles. Second, recent completion of genomic sequencing in model organisms has revealed the existence of *HS3ST* genes in invertebrate species including *C. elegans* and *Drosophila*, which differ greatly from mammals in their blood coagulation systems. Finally, 3-*O* sulfation of HS is suggested to be involved in the proliferation of various cancer cells (Miyamoto et al., 2003). These findings prompted us to reassess the roles of 3-*O* sulfated HS using in vivo systems. This approach was validated by our finding that the enzymatic sequence specificities of HS3STs are phylogenetically conserved. Most importantly, our work showed that reduction of *Hs3st-B* function using transgenic RNAi caused various morphological defects by compromising N signaling. This result demonstrated for the first time that 3-*O* sulfated HS controls a particular developmental pathway required for morphogenesis.

Mechanisms by which 3-*O* sulfated HS regulates *Drosophila* N signaling

What is the mechanism for control of the N signaling system by HS 3-*O* sulfation? Although our work implicated *Hs3st-B* in N signaling, there is no direct evidence reported to date of a requirement of HS in this pathway. However, there are several heparin-binding proteins that have been shown to regulate N signaling. Therefore, *Hs3st-B* may affect N activity through these molecules. First, Kuz, a *Drosophila* member of the ADAM family, has a domain that is highly conserved among members of the family. Because one of the mammalian homologues, ADAM12, was shown to interact with HS through this domain (Iba et al., 2000), Kuz could also potentially associate with HSPGs. Kuz cleaves the N^{ECD}, and this cleavage is required for activation of the N receptor (Lieber et al., 2002). Therefore, it is possible that 3-*O* sulfated HS interacts with Kuz and regulates the processing of N. The second candidate whose activity may be regulated by 3-*O* sulfated HS is Sca. Sca is a secreted fibrinogen-related protein that binds to heparin in vitro (Lee et al., 1996). Previous papers showed that Sca has an ability to directly bind and stabilize N protein on the cell surface (Powell et al., 2001). Finally, it is also possible that 3-*O* sulfated HS affects the N pathway through the activity of Wg, a known heparin-binding factor. It has been suggested that Wg binds to the specific EGF repeats of the N^{ECD}(Wesley, 1999) and that this binding inhibits interactions between N and its ligands, Dl and Ser, during development (Brennan et al., 1999). Therefore, 3-*O* sulfation of HS might control N signaling by modulating the N–Wg interaction.

Another model that explains how Hs3st-B regulates N protein levels was suggested by our experiments showing that *Hs3st-B* RNAi causes aberrant intracellular trafficking events. Previous work has shown that the activity of N signaling is very sensitive to alterations in membrane trafficking (for review see Baron et al., 2002). For example, *phosphocholine cytidylyltransferase 1* is involved in the formation of phospholipid membranes and positively regulates N signaling (Weber et al., 2003). *Phosphocholine cytidylyltransferase 1* mutant cells show an increase in endocytic activity and have enlarged endosomes, resulting in abnormal subcellular localization of N protein. In addition, mutations in *warthog*, which encodes a *Drosophila* homologue of rab6 and regulates trafficking from the Golgi to the trans-Golgi network, result in defective N signaling (Purcell and Artavanis-Tsakonas, 1999). Thus, some genes that are involved in controlling membrane trafficking are known to affect N signal transduction. Together with our observation, these findings suggest that a reduction of N protein by the *Hs3st-B* RNAi may be caused by abnormal sorting of N protein or enhanced activities of endocytosis/protein degradation. Interestingly, mammalian HS3ST-3 mediates the fusion of the viral envelope with the host cell membranes (Shukla et al., 1999), as well as the fusion between host cell membranes (Tiwari et al., 2004), suggesting a possible role of 3-*O* sulfated HS in membrane fusion during trafficking events. It is also possible that the *Hs3st-B* RNAi independently affects N signaling and intracellular trafficking.

Given that the role of HS in N signaling has not been reported, it is possible that the substrate of Hs3st-B is not HS, but other glycoconjugates such as sugar chains of N protein itself. The *O*-linked sugar chains on the EGF repeats of N protein play a key role in its activity (for review see Haines and Irvine, 2003), and further modification of this sugar chain (i.e., sulfation) may give a potential regulatory mechanism. It has been shown that *fringe* (*N*-acetylglucosaminyltransferase), *O-fucosyltransferase 1*, and *fringe connection* (UDP-sugar transporter) are involved in glycosylation of N and affect N signal transduction (for review see Haines and Irvine, 2003). Therefore, it is important to know the effects of *Hs3st-B* RNAi on modification of glycoconjugates other than HS. Also, we cannot rule out the possibility that *Hs3st-B* RNAi induces a phenomenon that does not reflect functions of endogenous HS chains. For example, inappropriately modified HS may exert an inhibitory effect on N signaling, even though HSPGs do not normally have any role in this pathway. Further studies on the function of

other HS biosynthetic enzymes and HSPG core protein genes in N signaling and membrane trafficking will reveal the molecular basis underlying the control of these events by 3-*O* sulfated HS. In particular, identification of the ligand of 3-*O* sulfated HS will be important to understand the in vivo functions of this class of enzymes.

Materials and methods

Fly stocks

The following mutant strains were used: N^{55e11} and N^{ts}, a null and a temperature-sensitive allele of *N*, respectively; Dl^{rev10}, a null allele of *Dl*; kuz^{e29-4}, a null allele of *kuz*; and dx^{1}, a temperature-sensitive allele of *dx*. The *lacZ* reporter lines used were as follows: vg^{BE}-*lacZ*, *vg* boundary enhancer; *neur-lacZ*; *E(spl)m8-lacZ*, *m8* gene from *E(spl)C*; N^{MLz}. The transgenic animals used were as follows: *UAS-sca*; *UAS-Dl*; *UAS-*N^{act}, a constitutively active form lacking the N^{ECD}; *UAS-GFP*; *actin-GAL4*; *GMR-GAL4*; *patched-GAL4*; *dpp-GAL4*. All aforementioned alleles and inserts are described in FlyBase (http://flybase.bio.indiana.edu). The transgenic RNAi animals used were as follows: *UAS-IR-Hs3st-*A^{M6}, *UAS-IR-Hs3st-*B^{M3}, and *UAS-IR-Hs3st-*B^{M6} (see also Construction of *Hs3st* transgenic RNAi flies). We used *UAS-IR-Hs3st-*B^{M3} to inhibit *Hs3st-B* function in all experiments unless stated otherwise in the text.

Cloning and enzymatic assay of Hs3sts

Two genomic loci for putative *Drosophila Hs3sts* (*Hs3st-A* ;CG33147, and *B*; CG7890) were identified in the *Drosophila* genome database using the tBlastn program of the BDGP. An *Hs3st-A* cDNA clone (GH20068) containing the entire protein coding region was obtained from the BDGP. To isolate an *Hs3st-B* cDNA clone, $\sim 4 \times 10^5$ colonies from a *Drosophila* embryonic cDNA library were screened using *Hs3st-B* genomic DNA as a probe (Brown and Kafatos, 1988). Hybridization was performed as described by Sambrook et al. (1989). One positive clone was isolated, and the inserted cDNA sequence was determined using a Big Dye™ Thermal Cycle Sequencing Ready Reaction Kit and the ABI PRISM 310 Analyzer.

To characterize the enzymatic sequence specificities of Hs3sts, expression constructs were generated by inserting an EcoRV–XhoI fragment of *Hs3st-A* and a HindIII–EcoRI fragment of *Hs3st-B* cDNAs into the polylinker of pcDNA3.1 (Life Technologies). pcDNA3.1-based expression plasmids containing mouse HS3ST-1 or human HS3ST-3_A were described previously (Shworak et al., 1997; Liu et al., 1999). Determination of CHO cell susceptibility to HSV-1 entry was performed as previously described (Montgomery et al., 1996; Shukla et al., 1999).

RT-PCR analyses

Total RNA was isolated from wild-type and *actin-GAL4/UAS-IR-Hs3st-B* larvae using the FastRNA Kit (BIO101) and FastPrep FP120 (BIO101). Isolated RNA was reverse-transcribed using SuperScript™ First-Strand Synthesis System for RT-PCR (Life Technologies). PCR experiments were performed using the synthesized cDNA as a template and the following primers: Hs3st-AFW (5′-GCTGCGATGACCACGACAAC-3′) and Hs3st-ARV (5′-TTCACCCGATGCTCAATGCC-3′) for *Hs3st-A* detection; Hs3st-BFW (5′-CTACTTCGTCACCAAGGAGG-3′) and Hs3st-BRV (5′-GCATAGACGCCGATCTTCAC-3′) for *Hs3st-B* detection; and rp49FW (5′-ATGACCATCCGCCCAGCATACAGG-3′) and rp49RV (5′-TCGTTCTCTTGAGAACGCAGGCGA-3′) for *ribosomal protein 49* detection.

Construction of *Hs3st* transgenic RNAi flies

Transgenic RNAi flies of *Hs3st-A* and *-B* were obtained using the inducible RNAi method (Kennerdell and Carthew, 2000). A 500-bp-long cDNA fragment from the first methionine was amplified by PCR and inserted as an IR into a modified pBluescript vector, pSC1, which possesses an IR formation site consisting of paired CpoI and SfiI restriction sites. In all cases, IRs were constructed in a head-to-head orientation. IR-containing fragments were cut out with NotI and were subcloned into pUAST, a transformation vector. Transformation of *Drosophila* embryos was performed using w^{1118} as a recipient strain.

Scanning EM

Adult flies were sequentially dehydrated in 25, 50, 75, and 100% ethanol, for 2 h each. The 100% dehydration was repeated three times. The preparation was subjected to critical point drying before being mounted on stubs and viewed on an S-4700 field emission scanning electron microscope (HITACHI).

In situ hybridization and immunostaining

In situ RNA hybridization was performed as described previously (Kamimura et al., 2001). Antibody staining was performed as described previously (Fujise et al., 2001) using rabbit anti–β-galactosidase (1:500; Cappel), mouse anti-Wg (4D4; 1:20; Developmental Studies Hybridoma Bank [DSHB]), mouse anti-Ct (2B10; 1:20; DSHB), mouse anti-N^{ECD} (C458.2H; 1:20; DSHB), mouse anti-N^{ICD} (C17.9C6; 1:10; DSHB), and mouse anti-Dl (C594.9B; 1:200). The primary antibodies were detected with Alexa Fluor–conjugated secondary antibodies (1:500; Molecular Probes).

Labeling the endosomal and lysosomal compartments

To visualize late endosomes, wing discs from third instar larvae were incubated in 0.5 mM of Texas red dextran (lysine fixable, MW3000; Molecular Probes) for 5 min in M3 medium at 25°C and then washed five times for 2 min with ice-cold M3 medium. Afterwards, these discs were incubated in M3 medium for 60 min at 25°C and fixed in PFA for 20 min at RT before mounting in VECTASHIELD Mounting Medium (Vector Laboratories). To visualize lysosomes, wing discs were incubated in 100 nM LysoTracker red (Molecular Probes) at 25°C for 2 min in PBS. Subsequently, the discs were washed two times with PBS and incubated in PBS at 25°C for 20 min. These discs were mounted in PBS for observation.

Online supplemental material

Fig. S1 shows the genetic interactions between *Hs3st-B* and various N signaling components during formation of the wing and notum. Online supplemental material is available at http://www.jcb.org/cgi/content/full/jcb.200403077/DC1.

We are grateful to S. Carroll, F. Schweisguth, K.D. Irvine, N.E. Baker, Y.N. Jan, T. Murata, S. Bray, K. Matsuno, the Developmental Studies Hybridoma Bank, and the Bloomington Stock Center for fly stocks and reagents. We thank T. Yabe for help with enzymatic analyses of Hs3st-B. We also thank S. Stringer, C. Kirkpatrick, and C. Firkus for critical reading of the manuscript and helpful comments.

This work was supported in part by the National Institutes of Health (grant HD042769 to H. Nakato and grant AI053774 to P.G. Spear) and the Human Frontier Science Program to H. Nakato and N.W. Shworak. K. Kamimura is supported by the Japan Society for the Promotion of Science for Young Scientists.

Submitted: 12 March 2004
Accepted: 12 August 2004

References

Artavanis-Tsakonas, S., M.D. Rand, and R.J. Lake. 1999. Notch signaling: cell fate control and signal integration in development. *Science.* 284:770–776.

Baron, M., H. Aslam, M. Flasza, M. Fostier, J.E. Higgs, S.L. Mazaleyrat, and M.B. Wilkin. 2002. Multiple levels of Notch signal regulation (review). *Mol. Membr. Biol.* 19:27–38.

Brand, A.H., and N. Perrimon. 1993. Targeted gene expression as a means of altering cell fates and generating dominant phenotypes. *Development.* 118:401–415.

Brennan, K., T. Klein, E. Wilder, and A.M. Arias. 1999. Wingless modulates the effects of dominant negative notch molecules in the developing wing of *Drosophila*. *Dev. Biol.* 216:210–229.

Brown, N.H., and F.C. Kafatos. 1988. Functional cDNA libraries from *Drosophila* embryos. *J. Mol. Biol.* 203:425–437.

Couso, J.P., E. Knust, and A. Martinez Arias. 1995. Serrate and wingless cooperate to induce vestigial gene expression and wing formation in *Drosophila*. *Curr. Biol.* 5:1437–1448.

de Celis, J.F., and S. Bray. 1997. Feed-back mechanisms affecting Notch activation at the dorsoventral boundary in the *Drosophila* wing. *Development.* 124: 3241–3251.

de Celis, J.F., J. de Celis, P. Ligoxygakis, A. Preiss, C. Delidakis, and S. Bray. 1996. Functional relationships between Notch, Su(H) and the bHLH genes of the E(spl) complex: the E(spl) genes mediate only a subset of Notch activities during imaginal development. *Development.* 122:2719–2728.

de Celis, J.F., S. Bray, and A. Garcia-Bellido. 1997. Notch signalling regulates veinlet expression and establishes boundaries between veins and interveins in

the *Drosophila* wing. *Development.* 124:1919–1928.

Doherty, D., G. Feger, S. Younger-Shepherd, L.Y. Jan, and Y.N. Jan. 1996. Delta is a ventral to dorsal signal complementary to Serrate, another Notch ligand, in *Drosophila* wing formation. *Genes Dev.* 10:421–434.

Esko, J.D., and S.B. Selleck. 2002. Order out of chaos: assembly of ligand binding sites in heparan sulfate. *Annu. Rev. Biochem.* 71:435–471.

Fehon, R.G., K. Johansen, I. Rebay, and S. Artavanis-Tsakonas. 1991. Complex cellular and subcellular regulation of notch expression during embryonic and imaginal development of *Drosophila*: implications for notch function. *J. Cell Biol.* 113:657–669.

Fujise, M., S. Izumi, S.B. Selleck, and H. Nakato. 2001. Regulation of dally, an integral membrane proteoglycan, and its function during adult sensory organ formation of *Drosophila*. *Dev. Biol.* 235:433–448.

Goto, S., M. Taniguchi, M. Muraoka, H. Toyoda, Y. Sado, M. Kawakita, and S. Hayashi. 2001. UDP-sugar transporter implicated in glycosylation and processing of Notch. *Nat. Cell Biol.* 3:816–822.

Haines, N., and K.D. Irvine. 2003. Glycosylation regulates Notch signalling. *Nat. Rev. Mol. Cell Biol.* 4:786–797.

HajMohammadi, S., K. Enjyoji, M. Princivalle, P. Christi, M. Lech, D. Beeler, H. Rayburn, J.J. Schwartz, S. Barzegar, A.I. de Agostini, M.J. Post, R.D. Rosenberg, and N.W. Shworak. 2003. Normal levels of anticoagulant heparan sulfate are not essential for normal hemostasis. *J. Clin. Invest.* 111:989–999.

Iba, K., R. Albrechtsen, B. Gilpin, C. Frohlich, F. Loechel, A. Zolkiewska, K. Ishiguro, T. Kojima, W. Liu, J.K. Langford, et al. 2000. The cysteine-rich domain of human ADAM 12 supports cell adhesion through syndecans and triggers signaling events that lead to β1 integrin–dependent cell spreading. *J. Cell Biol.* 149:1143–1156.

Kamimura, K., M. Fujise, F. Villa, S. Izumi, H. Habuchi, K. Kimata, and H. Nakato. 2001. *Drosophila* heparan sulfate 6-O-sulfotransferase (dHS6ST) gene. Structure, expression, and function in the formation of the tracheal system. *J. Biol. Chem.* 276:17014–17021.

Kennerdell, J.R., and R.W. Carthew. 2000. Heritable gene silencing in *Drosophila* using double-stranded RNA. *Nat. Biotechnol.* 18:896–898.

Kim, J., K.D. Irvine, and S.B. Carroll. 1995. Cell recognition, signal induction, and symmetrical gene activation at the dorsal-ventral boundary of the developing *Drosophila* wing. *Cell.* 82:795–802.

Kim, J., A. Sebring, J.J. Esch, M.E. Kraus, K. Vorwerk, J. Magee, and S.B. Carroll. 1996. Integration of positional signals and regulation of wing formation and identity by *Drosophila* vestigial gene. *Nature.* 382:133–138.

Kooh, P.J., R.G. Fehon, and M.A. Muskavitch. 1993. Implications of dynamic patterns of Delta and Notch expression for cellular interactions during *Drosophila* development. *Development.* 117:493–507.

Lecourtois, M., and F. Schweisguth. 1995. The neurogenic suppressor of hairless DNA-binding protein mediates the transcriptional activation of the enhancer of split complex genes triggered by Notch signaling. *Genes Dev.* 9:2598–2608.

Lee, E.C., X. Hu, S.Y. Yu, and N.E. Baker. 1996. The scabrous gene encodes a secreted glycoprotein dimer and regulates proneural development in *Drosophila* eyes. *Mol. Cell. Biol.* 16:1179–1188.

Lehmann, R., U. Dietrich, F. Jimenez, and J.A. Campos-Ortega. 1981. Mutations of early neurogenesis in *Drosophila. Wilhelm Roux's Archives of Developmental Biology.* 190:226–229.

Lehmann, R., F. Jimenez, U. Dietrich, and J.A. Campos-Ortega. 1983. On the phenotype and development of mutants of early neurogenesis in *Drosophila. Wilhelm Roux's Archives of Developmental Biology.* 192:62–74.

Lieber, T., S. Kidd, and M.W. Young. 2002. kuzbanian-mediated cleavage of *Drosophila* Notch. *Genes Dev.* 16:209–221.

Lindahl, U., M. Kusche-Gullberg, and L. Kjellen. 1998. Regulated diversity of heparan sulfate. *J. Biol. Chem.* 273:24979–24982.

Liu, J., Z. Shriver, P. Blaiklock, K. Yoshida, R. Sasisekharan, and R.D. Rosenberg. 1999. Heparan sulfate D-glucosaminyl 3-O-sulfotransferase-3A sulfates N-unsubstituted glucosamine residues. *J. Biol. Chem.* 274:38155–38162.

Micchelli, C.A., E.J. Rulifson, and S.S. Blair. 1997. The function and regulation of cut expression on the wing margin of *Drosophila*: Notch, Wingless and a dominant negative role for Delta and Serrate. *Development.* 124:1485–1495.

Miyamoto, K., K. Asada, T. Fukutomi, E. Okochi, Y. Yagi, T. Hasegawa, T. Asahara, T. Sugimura, and T. Ushijima. 2003. Methylation-associated silencing of heparan sulfate D-glucosaminyl 3-O-sulfotransferase-2 (3-OST-2) in human breast, colon, lung and pancreatic cancers. *Oncogene.* 22:274–280.

Montgomery, R.I., M.S. Warner, B.J. Lum, and P.G. Spear. 1996. Herpes simplex virus-1 entry into cells mediated by a novel member of the TNF/NGF receptor family. *Cell.* 87:427–436.

Mumm, J.S., and R. Kopan. 2000. Notch signaling: from the outside in. *Dev. Biol.* 228:151–165.

Nakato, H., and K. Kimata. 2002. Heparan sulfate fine structure and specificity of proteoglycan functions. *Biochim. Biophys. Acta.* 1573:312–318.

Panin, V.M., and K.D. Irvine. 1998. Modulators of Notch signaling. *Semin. Cell Dev. Biol.* 9:609–617.

Powell, P.A., C. Wesley, S. Spencer, and R.L. Cagan. 2001. Scabrous complexes with Notch to mediate boundary formation. *Nature.* 409:626–630.

Purcell, K., and S. Artavanis-Tsakonas. 1999. The developmental role of warthog, the notch modifier encoding Drab6. *J. Cell Biol.* 146:731–740.

Rosenberg, R.D., N.W. Shworak, J. Liu, J.J. Schwartz, and L. Zhang. 1997. Heparan sulfate proteoglycans of the cardiovascular system. Specific structures emerge but how is synthesis regulated? *J. Clin. Invest.* 99:2062–2070.

Rulifson, E.J., and S.S. Blair. 1995. Notch regulates wingless expression and is not required for reception of the paracrine wingless signal during wing margin neurogenesis in *Drosophila*. *Development.* 121:2813–2824.

Sambrook, J., E.F. Fritsch, and T. Maniatis. 1989. Screening of bacterial colonies for recombinant plasmids. Molecular Cloning: A Laboratory Manual. Second edition. Cold Spring Harbor Laboratory Press, Cold Spring Harbor, NY. 1.90–1.104.

Shukla, D., J. Liu, P. Blaiklock, N.W. Shworak, X. Bai, J.D. Esko, G.H. Cohen, R.J. Eisenberg, R.D. Rosenberg, and P.G. Spear. 1999. A novel role for 3-O-sulfated heparan sulfate in herpes simplex virus 1 entry. *Cell.* 99:13–22.

Shworak, N.W., J. Liu, L.M.S. Fritze, J.J. Schwartz, L. Zhang, D. Logeart, and R.D. Rosenberg. 1997. Molecular cloning and expression of mouse and human cDNAs encoding heparan sulfate D-glucosaminyl 3-*O*-sulfotransferase. *J. Biol. Chem.* 272:28008–28019.

Shworak, N.W., J. Liu, L.M. Petros, L. Zhang, M. Kobayashi, N.G. Copeland, N.A. Jenkins, and R.D. Rosenberg. 1999. Multiple isoforms of heparan sulfate D-glucosaminyl 3-O-sulfotransferase. Isolation, characterization, and expression of human cdnas and identification of distinct genomic loci. *J. Biol. Chem.* 274:5170–5184.

Simpson, P. 1990. Notch and the choice of cell fate in *Drosophila* neuroepithelium. *Trends Genet.* 6:343–345.

Tiwari, V., C. Clement, M.B. Duncan, J. Chen, J. Liu, and D. Shukla. 2004. A role for 3-O-sulfated heparan sulfate in cell fusion induced by herpes simplex virus type 1. *J. Gen. Virol.* 85:805–809.

Ueda, R. 2001. Rnai: a new technology in the post-genomic sequencing era. *J. Neurogenet.* 15:193–204.

Warner, M.S., R.J. Geraghty, W.M. Martinez, R.I. Montgomery, J.C. Whitbeck, R. Xu, R.J. Eisenberg, G.H. Cohen, and P.G. Spear. 1998. A cell surface protein with herpesvirus entry activity (HveB) confers susceptibility to infection by mutants of herpes simplex virus type 1, herpes simplex virus type 2, and pseudorabies virus. *Virology.* 246:179–189.

Weber, U., C. Eroglu, and M. Mlodzik. 2003. Phospholipid membrane composition affects EGF receptor and Notch signaling through effects on endocytosis during *Drosophila* development. *Dev. Cell.* 5:559–570.

Wesley, C.S. 1999. Notch and wingless regulate expression of cuticle patterning genes. *Mol. Cell. Biol.* 19:5743–5758.

Xia, G., J. Chen, V. Tiwari, W. Ju, J.P. Li, A. Malmstrom, D. Shukla, and J. Liu. 2002. Heparan sulfate 3-O-sulfotransferase isoform 5 generates both an antithrombin-binding site and an entry receptor for herpes simplex virus, type 1. *J. Biol. Chem.* 277:37912–37919.

Yabe, T., D. Shukla, P.G. Spear, R.D. Rosenberg, P.H. Seeberger, and N.W. Shworak. 2001. Portable sulphotransferase domain determines sequence specificity of heparan sulphate 3-O-sulphotransferases. *Biochem. J.* 359:235–241.